Structural and Dynamic Evidence for C−H···O Hydrogen Bonding in Lariat Ethers: Implications for Protein Structure

Eric S. Meadows,[†] Stephen L. De Wall,[†] Leonard J. Barbour,[‡] Frank R. Fronczek,[§] Min-Sook Kim, and George W. Gokel*[,†]

Contribution from the Bioorganic Chemistry Program & Department of Molecular Biology & Pharmacology, Washington University School of Medicine, 660 S. Euclid Avenue, Campus Box 8103, St. Louis, Missouri 63110, Department of Chemistry, University of Missouri, 601 South College Avenue, Columbia, Missouri 65211, and Department of Chemistry, Louisiana State University, Baton Rouge, Louisiana 70809-1804

Received November 19, 1999

Abstract: Seven diaza-18-crown-6 ethers having aromatic sidearms were studied: benzyl (**1**), 2-hydroxybenzyl (**2**), dansyl (**3**), 1-naphthylmethyl (**4**), 2-naphthylmethyl (**5**), 9-anthrylmethyl (**6**), and 1-pyrenylmethyl (**7**). Solution studies of these compounds included homogeneous binding constant determination, picrate extraction efficiency, and/or bulk chloroform membrane transport rate experiments. Compounds **2**, **3**, **4**, **6**, and **7** exhibited binding affinities for alkali metal cations that were surprisingly low. Fifteen crystal structures have been used to understand the conformations of **1**−**7** and their alkali metal complexes. Unusually weak cation binding in solution was found to correlate with intramolecular interactions observed between the crown's macroring and both sidearms. For one of the five weakly binding crowns (**2**) the low binding affinity is attributed to an intramolecular O−H···N hydrogen bond, confirmed by the solid-state structure and IR studies. The weak cation binding abilities of **3**, **4**, **6**, and **7** are ascribed to intramolecular C−H···O contacts that appear to define both structure and binding affinity. A total of ten C−H···O hydrogen bonds are observed in seven of the solid-state structures. Unusual conformations, dominated by intramolecular aromatic−oxygen interactions, are observed in cases that involve C−H···O hydrogen bond formation. The observed C−H···O contacts are paralleled in proteins, where a crystal structure of myoglobin exhibits an analogous interaction.

Introduction

The macrocycles that Pedersen named crown ethers[1] and their numerous structural variants[2] have now been known for more than three decades. During this period, these compounds have been studied extensively, especially as cation complexing agents.[3] Many research groups have reported the structures and properties of numerous macrocycles, free and with bound metallic cations, organic cations, and neutral species.[4] Despite the extensive study and application of crowns, novel and unanticipated properties continue to emerge.

A more recent and emerging application of macrocycles is as low molecular weight receptors to be used in assessing noncovalent interactions that are important in chemistry and biology.[5,6] Such model systems have several distinct advantages over the native biological macromolecules. First, high resolution structural data are often accessible for the synthetic receptors. Second, virtually endless, systematic structural modifications can be made to model systems by the application of synthetic organic chemistry. Natural biopolymers are generally limited to specific substitutions (site directed mutagenesis) or deletions in the primary sequence. It is also possible to incorporate unnatural side chains in proteins[7,8] but the technical challenges are daunting.

The relative simplicity of an appropriate model system allows for specific interactions to be isolated and studied in the absence of the many other interactions that may be present in biological macromolecules. When the interesting or sought after chemical properties are observed in the synthetic receptor systems, it may be inferred that the chemistry is equally applicable to biomolecules even though the latter are normally more complex structures. Verification of unusual properties in synthetic receptor systems and the general extensibility of the chemistry can give insight into the biological implications for such chemical interactions.

Our efforts reported here involve model systems originally designed to be fluorescent, cation-sensing probes. Recent reports by Kubo and co-workers involved *N*,*N*′-bis(1-naphthylmethyl)-

[†] Washington University School of Medicine.
[‡] University of Missouri.
[§] Louisiana State University.

(1) Pedersen, C. J. *J. Am. Chem. Soc.* **1967**, *89*, 7017.

(2) Gokel, G. W.; Korzeniowski, S. H. *Macrocyclic Polyether Syntheses*; Springer-Verlag: Berlin, 1982; 415 pp.

(3) (a) Izatt, R. M.; Pawlak, K.; Bradshaw, J. S.; Bruening, R. L. *Chem. Rev.* **1995**, *95*, 2529−2586. (b) Inoue, Y.; Gokel, G. W. *Cation Binding by Macrocycles*; Marcel Dekker: New York, 1990; 761 pp. (c) Gokel G. W., Ed. Molecular Recognition: Receptors for Cationic Guests. In *Comprehensive Supramolecular Chemistry*; Elsevier Science: Oxford, 1996; Vol. 1, 850 pp.

(4) (a) Hiraoka, H. *Crown compounds: their characteristics and applications*; Amsterdam: Elsevier Scientific Publishing Co., 1982. (b) Gokel, G. W. *Crown ethers and cryptands*; Royal Society of Chemistry: Cambridge, 1991; Vol. 3. (c) Cox, B. G.; Schneider, H. *Coordination and Transport Properties of Macrocyclic Compounds in Solution*; Elsevier: Amsterdam, 1992. (d) Dietrich, B.; Viout, P.; Lehn, J.-M. *Macrocyclic Chemistry*; VCH Publishers: Weinheim, 1993.

(5) (a) De Wall, S. L.; Meadows, E. S.; Barbour, L. J.; Gokel, G. W. *J. Am. Chem. Soc.* **1999**, *121*, 5613−4. (b) De Wall, S. L.; Barbour, L. J.; Gokel, G. W. *J. Am. Chem. Soc.* **1999**, *121*, 8405−6.

(6) Schall, O. F.; Gokel, G. W. *J. Org. Chem.* **1996**, *61*, 1449−1458.

(7) Wilken, J.; Kent, S. B. H. *Curr. Opin. Biotechnol.* **1998**, *9*, 412−426.

(8) Mendel, D.; Cornish, V. W.; Schultz, P. G. *Annu. Rev. Biophys. Biomol. Struct.* **1995**, *24*, 435−462.

10.1021/ja9940672 CCC: $19.00
Published on Web 03/24/2000

4,13-diaza-18-crown-6 (**4**),[9] *N*,*N*′-bis(9-anthrylmethyl)-4,13-diaza-18-crown-6 (**6**),[10] and *N*,*N*′-bis(1-pyrenylmethyl)-4,13-diaza-18-crown-6 (**7**)[11] for use as fluorescent, cation sensors. Surprisingly, the observed cation binding strengths and corresponding fluorescence changes were quite modest. Our own poor level of success using the dansyl residue[12] (**3**) in a similar fashion prompted us to study the situation more carefully. We now report solid-state structures and complexation behavior for a family of 4,13-diaza-18-crown-6 derivatives. We have found that in these systems, poor cation interactions correlate with intramolecular hydrogen bond formation, either of the traditional type or involving C−H···O contacts. Finally we show that the information gleaned from this study has implications for biological systems.

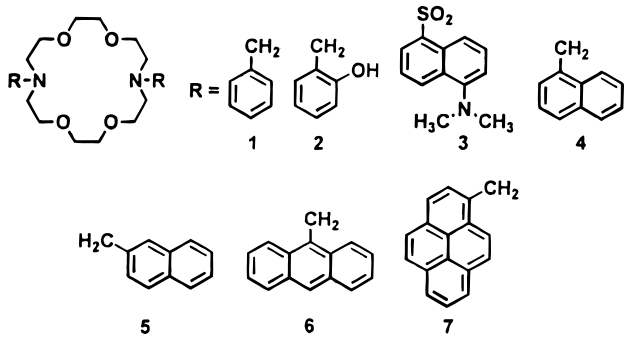

C−H···O Interactions. The importance of C−H···O interactions has been debated, at times fiercely,[13] since Sutor first postulated their existence based on crystallographic studies.[14] Even before Sutor's noteworthy report, C−H···O interactions were proposed to explain trends in pK_A values of carboxylic acids.[15] More recently, C−H···O interactions have been observed in the crystal structures of amino acids,[16] proteins,[17] protein−ligand complexes,[18] and DNA structures.[19] These types of interactions have also been referred to as "aromatic-oxygen interactions".[20] Desiraju has recently discussed the occurrence of C−H···O interactions in a variety of structural settings.[21] He has used the letter "*D*" to design the C···O contact distance and noted that *D* values within the range of 3.00−4.00 Å can be "significant." The conventional designations of *D*, *d*, and θ are shown in the schematic. He has further observed that "linear

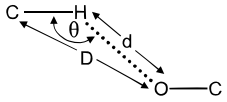

bonds ($150° \leq \theta \leq 180°$) are structurally significant". The positions of the carbon and oxygen atoms are generally observed more accurately than hydrogen atoms in X-ray crystal structures. Thus the C···O distance, *D*, is often preferred over the H···O distance, *d*, as the span used for comparisons between structures.

Although these "hydrogen bonds" are now well recognized, their role in determining conformation is not as well established. As recently as 1991, it was stated that "...hydrogen bonds with C−H as donor will not have a major influence on molecular conformation."[22] Any C−H···O contact must be of sufficient energy if it is to affect molecular conformation. The calculated interaction energies of such simple systems as CH_4···OH_2 have been the subject of disagreement. One report[23] suggests that the calculated ab initio binding energies are not very dependent on the basis set. However, the authors found that, when 6-31G*, 6-311G**, or 6-311G(2d,p) basis sets were used, electron correlation (MP2 and MP4) gave calculated CH_4···OH_2 binding energies that were approximately 1 kcal/mol greater. A more recent report[24] confirmed the lack of sensitivity to the basis set but also found little difference between the correlated methods (MP2, MP4, QCISD, and CCSD-(T)), at least when using the 6-31+G** basis set. Currently, the range of calculated binding energies for CH_4···OH_2 is 0.3−1.9 kcal/mol.

Results and Discussion

Compounds Prepared. *N*,*N*′-Dibenzyl-4,13-diaza-18-crown-6 (**1**) has been extensively studied and serves as a benchmark in the diaza-18-crown-6 series. Compared to **1**, we noted a surprising lack of binding affinity for the *o*-hydroxybenzyl analogue (**2**) and *N*,*N*′-didansyl-4,13-diaza-18-crown-6 (**3**). Compound **2** was devised originally in an effort to use the deprotonated *o*-hydroxyl groups as "intramolecular anions" in the three-dimensional coordination of alkali metal cations. Dansyl compound **3** was prepared in the hope that it would serve as a fluorescent carrier molecule that could be used to probe the lipid bilayer environment. Although the fluorescent properties of didansyl crown **3** were as expected, the binding constants for Na^+ and K^+ by either **2** or **3** were poor. In fact, we could not detect any Na^+ or K^+ complexation by didansyl crown **3** using any of several methods for determining alkali metal cation binding affinity. The methods attempted were (1) bulk membrane transport, (2) picrate extraction, and (3) binding constant measurements using ion selective electrode methods.

In an effort to understand the failure of didansyl crown **3** to serve as a fluorescent carrier molecule we selected molecules **4**−**7** for comparison. We recently reported solid-state structures for naphthylmethyl crowns **4** and **5**[25] and anthrylmethyl crown

(9) Kubo, K.; Ishige, R.; Kato, N.; Yamamoto, E.; Sakurai, T. *Heterocycles* **1997**, *45*, 2365−2379.
(10) Kubo, K.; Ishige, R.; Sakurai, T. *Heterocycles* **1998**, *48*, 347−351.
(11) Kubo, K.; Kato, N.; Sakurai, T. *Acta Crystallogr.* **1997**, *C53*, 132−134.
(12) Meadows, E. S.; De Wall, S. L.; Salama, P. W.; Abel, E.; Gokel, G. W. *Supramol. Chem.* **1999**, *10*, 163−171.
(13) Donohue, J. In *Structural Chemistry and Molecular Biology*; Rich, A., Davidson, N., Eds.; W. H. Freeman: San Francisco, 1968; pp 459−463.
(14) Sutor, D. J. *Nature* **1962**, *195*, 68−69.
(15) Dippy, J. F. J. *Chem. Rev.* **1939**, *25*, 151−205.
(16) Jeffrey, G. A.; Maluszynska, H. *Int. J. Biol. Micromol.* **1982**, *4*, 173−185.
(17) (a) Zygmunt S.; Lee, L.; Derewenda, U. *J. Mol. Biol.* **1995**, *252*, 248−262. (b) Bella, J.; Berman, H. M. *J. Mol. Biol.* **1996**, *264*, 734−742.
(18) (a) Hovey, B. T.; Verlinde, C. L. M. J.; Merrit, E. A.; Hol, W. G. J. *J. Mol. Biol.* **1999**, *285*, 1169−1178. (b) Gray, N. S.; Wodicka, L.; Thunnissen, A.-M. W. H.; Norman, T. C.; Kwon, S.; Espinoza, F. H.; Morgan, D. O.; Barnes, G.; LeClerc, S.; Meijer, L.; Kim, S.-H.; Lockhart, D. J.; Schultz, P. G. *Science* **1998**, *281*, 533−538. (c) Perutz, M. F.; Fermi, G.; Abraham, D. J.; Poyart, C.; Bursaux, E. *J. Am. Chem. Soc.* **1986**, *108*, 1064−1078.
(19) (a) Mandel-Gutfreund, Y.; Margalit, H.; Jernigan, R. L.; Zhurkin, V. B. *J. Mol. Biol.* **1998**, *277*, 112−1140. (b) Takahara, P. M.; Frederick, C. A.; Lippard, S. J. *J. Am. Chem. Soc.* **1996**, *118*, 12309−12321.
(20) (a) Burley, S. K.; Petsko, G. A. *Adv. Protein Chem.* **1988**, *39*, 125−189. (b) Gould, R. O.; Gray, A. M.; Taylor, P.; Walkinshaw, M. D. *J. Am. Chem. Soc.* **1985**, *107*, 5921−5927. (c) Thomas, K. A.; Smith, G. M.; Thomas, T. B.; Feldmann, R. J. *Proc. Natl. Acad. Sci. U.S.A.* **1982**, *79*, 4843−4847.
(21) Desiraju, G. R. *Acc. Chem. Res.* **1996**, *29*, 441−449.
(22) Jeffrey, G. A.; Saenger, W. In *Hydrogen Bonding in Biological Structures*; Springer-Verlag: Berlin, 1991; p 156.
(23) Seiler, P.; Weisman, G. R.; Glendening, E. D.; Weinhold, F.; Johnson, Van. B.; Dunitz, J. D. *Angew. Chem., Int. Ed. Engl.* **1987**, *26*, 1175−1177.
(24) Gu, Y.; Kar, T.; Scheiner, S. *J. Am. Chem. Soc.* **1999**, *121*, 9411−9422.
(25) Meadows, E. S.; De Wall, S. L.; Barbour, L. J.; Gokel, G. W. *Chem. Commun.* **1999**, *16*, 1555−1556.

Table 1. Log K_S Values for *N,N′*-Diaryl-4,13-diaza-18-crown-6 in Methanol at 25 °C[a]

	arene sidearms on 4,13-diaza-18-crown-6				
added salt	benzyl (**1**)	*o*-hydroxybenzyl (**2**)	1-naphthylmethyl (**4**)	2-naphthylmethyl (**5**)	anthrylmethyl (**6**)
NaCl	2.71 ± 0.02	2.42	2.32 ± 0.26	2.68 ± 0.10	*b*
NaI	2.50 ± 0.11		1.87 ± 0.17	2.37 ± 0.11	*b*
NaSCN[d]			2.09 ± 0.04		*b*
NaSCN[a,d]					2.70 ± 0.1[a]
KI ($n = 1$)[c]	3.55 ± 0.03			3.50 ± 0.02	*b*
KCl	3.38 ± 0.02	2.59			*b*
KSCN[d]			3.27 ± 0.07		*b*
KSCN[a,d]			3.45 ± 0.02[a]		3.29 ± 0.13[a]

[a] Except where noted: 9:1 $CH_3OH/CHCl_3$. [b] Insoluble in CH_3OH. [c] Stoichiometry calculated for data fit in the isothermal titration calorimetry experiment (see Experimental Section). [d] Measured by Kubo et al.[9,10]

6.[26] The 1-naphthylmethyl compound, **4**, was intended to incorporate the aromatic rings of **3** but without the 5-dimethylamino group or the sulfonamide linker. The 2-naphthylmethyl crown, **5**, is isomeric with **4** and can be used to determine the importance of the aromatic ring orientation with respect to the crown. Compounds **6** and **7** incorporate anthryl and pyrenyl sidearms, respectively. These sidearms are, like dansyl, fluorescent and they provide a means for assessing the effect, if any, of increasing the size of the aromatic appendages.

Compound Syntheses. All of the compounds described in this study have been previously reported. Procedures were developed in our laboratory for the preparations of *N,N′*-bis(benzyl)-4,13-diaza-18-crown-6 (**1**),[27] *N,N′*-bis(2-hydroxybenzyl)-4,13-diaza-18-crown-6 (**2**),[28] *N,N′*-bis(dansyl)diaza-18-crown-6 (**3**),[12] and *N,N′*-bis(2-naphthylmethyl)-4,13-diaza-18-crown-6 (**5**).[25] The two-armed diaza-18-crown-6 derivatives having 1-naphthylmethyl (**4**),[9] 9-anthrylmethyl (**6**),[10] or 1-pyrenylmethyl (**7**)[11] were prepared first by Kubo and co-workers.

Structure and Cation Binding Properties of *N,N*-Bis(2-hydroxybenzyl)diaza-18-crown-6 (2). Dibenzyldiaza-18-crown-6 (**1**) has been extensively studied during the two decades since it was originally prepared.[29] A comparison of Na^+ and K^+ cation binding by it and the *o*-hydroxybenzyl derivative, **2**, provides an interesting contrast. In methanol solution, binding constants (log K_S) for dibenzyl crown (**1**) are 2.72 (Na^+) and 3.38 (K^+) as shown in Table 1. The corresponding values for hydroxybenzyl crown **2** are 2.42 (Na^+) and 2.59 (K^+). These values are expressed as decadic logarithms so the difference in K^+ binding constants is nearly a power of ten. The relative of **1** and **2**, *N,N′*-bis(2-methoxybenzyl)-4,13-diaza-18-crown-6, exhibits binding constants as follows: 3.65 (Na^+) and 4.94 (K^+).[22] The latter values are much higher than the unsubstituted benzyl compound because the *o*-oxygens are well positioned to provide additional solvation for the ring-bound cation. The difference between the *o*-methoxy and *o*-hydroxy derivatives is more than 10-fold for Na^+ and more than 100-fold for K^+.

The difference in cation binding strengths for **2** and *N,N′*-bis(2-methoxybenzyl)-4,13-diaza-18-crown-6 is remarkable. It can be understood, however, in terms of the crystal structures of two-armed (bibracchial) lariat ethers. For example, the K^+ ion, when complexed by *N,N′*-bis(2-methoxyethyl)-4,13-diaza-18-crown-6, is 8-coordinate: the sidearm oxygen atoms provide apical coordination for the ring-bound cation. This is also the case for the Na^+ and K^+ complexes of *N,N′*-bis(2-methoxy-1-naphthyl)-4,13-diaza-18-crown-6 reported by Wang and co-workers.[30] Superficially, the *o*-hydroxybenzyl derivative (**2**) is also expected to coordinate cations utilizing the oxygen donor atom present in the sidearm. The solid state structure accounts clearly for the surprising lack of binding strength: the hydroxyl groups in **2** form N···H−O hydrogen bonds that involve four of the eight potential donor groups. The remaining donor groups are either blocked or sterically hindered by the position of the arene enforced by the H-bonding arrays. The structure of **2** is shown in Figure 1 (panel B) along with the structure of uncomplexed **1** (panel A). The latter exhibits the expected unbound crown conformation and the two benzyl sidearms are turned away from the macroring. The contrast with the sidearm orientation of **2** is striking.

Additional evidence for H-bond formation was obtained by infrared analysis of *o*-hydroxybenzyl crown **2**. A sample of solid **2** in a KBr matrix showed a hydroxyl vibration at $\nu_{OH} = 3100$ cm^{-1}. A sample of **2** dissolved in $CDCl_3$ showed a strong absorption band at 3060 cm^{-1}. In contrast, the hydroxyl vibration of 4-hydroxybenzaldehyde is reported to occur at $\nu_{OH} = 3600$ cm^{-1}. The isomer, 2-hydroxybenzaldehyde, is known to form an intramolecular hydrogen bond and its hydroxyl vibration is observed at $\nu_{OH} = 3077$ cm^{-1}. Thus, the infrared analysis agrees with the intramolecularly H-bonded structure shown for **2** in Figure 1.

Comparison of *N,N*-Bis(dansyl)-4,13-diaza-18-crown-6 (3) and *N,N*-Bis(2-hydroxybenzyl)-4,13-diaza-18-crown-6 (2). We have recently reported[12] that the Na^+ and K^+ binding constants for dansyl crown **3** in CH_3OH solution are too low to measure. In addition, an attempt was made to assess alkali metal cation transport using the concentric tube/picric acid technique.[31] This is a standard technique in which two aqueous phases are separated by a layer of chloroform that constitutes an organic membrane. The water and $CHCl_3$ (bottom phase) are placed in a beaker. A glass tube is inserted coaxial with the beaker's long axis. The glass tube does not reach the bottom of the $CHCl_3$ phase but it does separate the aqueous phase into inner and outer rings. The ionophore in question is added to the membrane ($CHCl_3$) and transport of Na^+ from the source phase (inner ring) to the receiving aqueous phase is monitored by colorimetric analysis by UV spectroscopy of the yellow picrate anion. No cation transport could be detected for **3** by this relatively sensitive technique.

A limitation of any comparison involving **3** as a cation binder is that the electron density on both of its macroring nitrogens is diminished by the sulfonamide groups. Thus, **3** has four ether oxygen donors available for cation complexation. A CPK molecular model of **3** suggested that Na^+ could be coordinated

(26) De Wall, S. L.; Meadows, E. S.; Barbour, L. J.; Gokel, G. W. *Chem. Commun.* **1999**, *16*, 1553−1554.
(27) Gatto, V. J.; Miller, S. R.; Gokel, G. W. *Org. Synth.* **1990**, *68*, 227−33.
(28) Gatto, V. J.; Gokel, G. W. *J. Am. Chem. Soc.* **1984**, *106*, 8240−8244.
(29) Wester, N.; Vögtle, F.; *J. Chem. Res.* **1978**, *10*, 400−401.
(30) Wang, D.; Ge, Y.; Hu, H.; Yu, K.; Zhao, Z. *J. Chem. Soc., Chem. Commun.* **1991**, 685−687.
(31) Hernandez, J. C.; Trafton, J. E.; Gokel, G. W. *Tetrahedron Lett.* **1991**, 6269−6270.

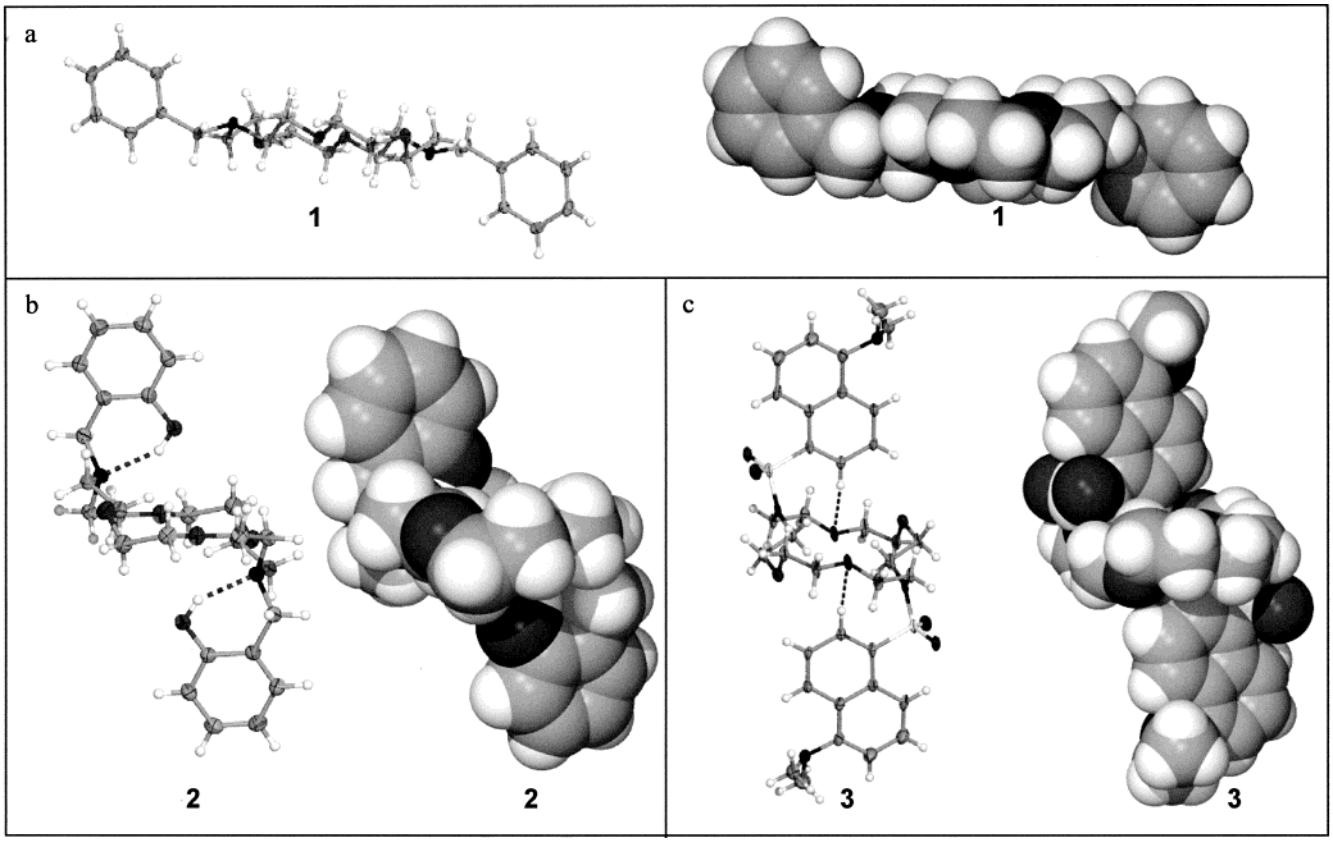

Figure 1. Thermal ellipsoid (left) and space filling (right) plots of **1** (a), **2** (b), and **3** (c). The ellipsoid plots are drawn at the 50% probability level.

by six oxygens (four provided by the macroring and two sulfonamide oxygens on one sidearm). However, in the conformation observed in the crystal structure of **3**, the sulfonyl donors are unavailable for complexation.

The solid-state structure of dansyl crown **3** (shown in Figure 1c) bears a remarkable similarity to that of hydroxybenzyl crown **2** despite the absence of any obvious OH or NH donor. The essentially identical conformations of **2** and **3** are apparent in Figure 2 in which framework diagrams are overlaid in both side (Figure 2a) and top views (Figure 2b). In the case of **2**, the H-bond interaction is obvious and traditional. The solid-state structure of pyrenyl crown **7** (see below) is shown in side (Figure 2c) and top (Figure 2d) views because of the remarkable similarity with **2** and **3**. In **3** and **7**, the stabilizing intramolecular interaction is a C−H···O, rather than N···H−O (as in **2**), hydrogen bond interaction that apparently helps to define the conformation of the noncomplexed macrocycle.

The close contact in **3** is observed between a naphthalene C−H and the macroring oxygen atom (D = 3.36 Å, d = 2.49 Å). The angle (θ) is 157.2°. This C−H···O interaction, observed in dansyl crown **3**, is significant by Desiraju's geometric criteria, but more important, the chemical behavior of this compound may be affected as a result.

Comparison of Pyrenyl Crown 7 with 2 and 3. The solid-state structure of compound **7** was reported by Kubo and co-workers[11] (see Figure 2c,d). To our knowledge, it is the only other example of an uncomplexed, disubstituted crown that exhibits a solid-state conformation similar to that of **2** and **3**. This structure is included because it was determined independently and reported separately from any efforts of ours. There is no discussion of C−H···O hydrogen bonding in Kubo's report but the similarity of the conformation, distances, and angles is striking. Thus, the H···O distance, d (dashed line in Figure 2c), is 2.58 (D = 3.50 Å). The angle, θ, is 168.3°. If related interactions are not involved in all cases, the structural similarity between **2**, **3**, and **7** is an astonishing coincidence. It is interesting to note that the complexation ability of **7** reported by Kubo and co-workers was also poor, within experimental error of the binding constants (shown below) for the related dianthryl crown (**6**).

Cation Transport by Naphthyl- and Anthryl-Sidearmed Diazamacrocycles. The evaluation of properties began by assessing the abilities of **1** and **3**−**6** to transport sodium picrate through a bulk chloroform membrane (see above and Experimental Section). The values obtained for Na^+ transport experiments by **1**, **3**, **4**, **5**, and **6** are shown in the graph of Figure 3. Each bar represents a minimum of four replicates and some were run as many as 15 times.

Dibenzyldiaza-18-crown-6 (**1**) serves as a control for the compounds studied. Given the error limits of these experiments, the observed transport rates for benzyl crown **1** and 2-naphthyl crown **5** are similar. It is interesting to note that the 2-naphthylmethyl sidearm is more structurally similar to benzyl than to **3** (dansyl), **4** (1-naphthylmethyl), or **6** (1-anthrylmethyl), i.e. there is no peri interaction at the point of attachment. When the naphthylmethyl sidearm is attached to the arene's 1-position (**4**) rather than the 2-position (**5**), Na^+ transport drops to about half of the previous value. Fusion of another aromatic ring onto the sidearm [i.e. 1-naphthyl (**4**) → 9-anthryl (**6**)] further reduces sodium transport. Cation transport by didansyldiaza-18-crown-6 was so low that it could hardly be measured but this sulfonic acid derivative may be the least comparable system in the present study.

Homogeneous Cation Complexation Strengths. We have previously shown that there is a reasonable correlation between cation binding constants and transport assessed by the concentric tube/picrate method.[31] To confirm the surprising transport results detailed above, we determined homogeneous cation complex-

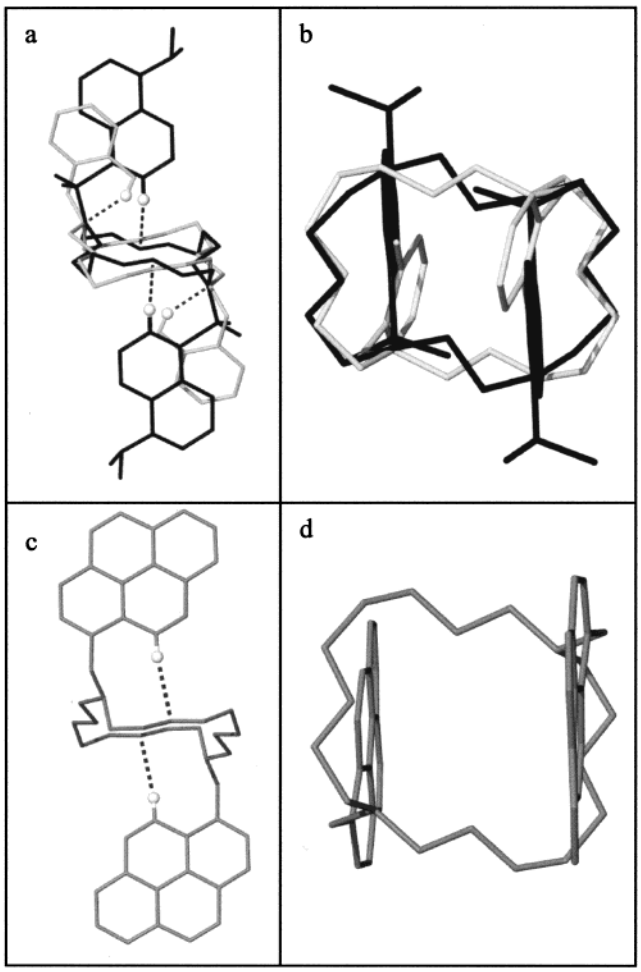

Figure 2. Comparison of solid-state structures. (a) Side view of **2** (light) and **3** (dark) overlaid; (b) top view of **2** (light) and **3** (dark) overlaid; (c) side view of **7**; and (d) top view of **7**. The structure of **7** is taken from entry TERXUJ[11] from the CCSD.

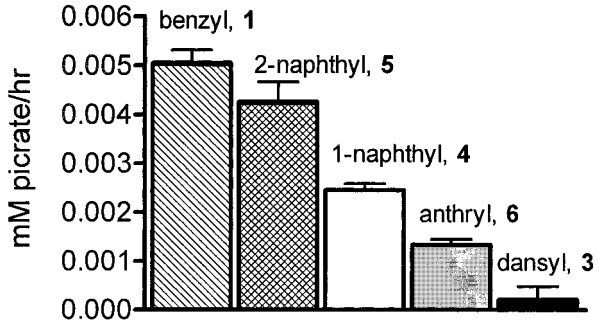

Figure 3. Sodium picrate transport rates for **1**, **3**, **4**, **5**, and **6**.

ation constants for the benzyl (**1**) and naphthyl crowns (**4**, **5**). We had previously determined log K_S for **2** but we were unable to obtain a complexation constant for dansyl crown **3** because its binding to either Na^+ or K^+ (MeOH, 25 °C) was too weak. An additional problem was the poor solubility of dansyl-sidearmed **3** in methanol; this was also the case for anthryl-methyl-sidearmed **6**.

The data recorded in Table 1 were obtained by fluorescence, isothermal titration calorimetry, or ion selective electrode methods. Fluorescence methods were preferred in cases in which the solubility of the host molecule was low and calorimetry was utilized when additional thermodynamic data were required. In some cases, two or three methods were used for the same combination of cation and host and the values are all expressed

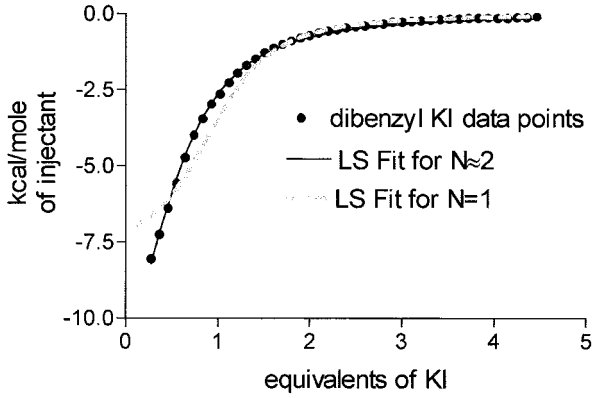

Figure 4. Binding isotherm for **1**·K^+ as measured by ITC.

in Table 1 within the specified error limits. The results shown for **6** were determined by Kubo et al. in $CH_3OH/CHCl_3$ (9:1).[9,10]

Cation binding constants (log K_S, 25 °C, CH_3OH, Cl^- anion) for Na^+ and K^+ have previously been determined for dibenzyl crown **1** by ion selective electrode (ISE) methods:[32] 2.68 (Na^+) and 3.38 (K^+). The literature values and the binding constants reported here are in reasonable agreement. Complexation of Na^+ and K^+ by **1** was assessed by isothermal titration calorimetry (ITC) to compare it with the values obtained by ISE. The data acquired by this method were reproducible and consistent with values obtained by other methods. The calorimeter's internal data analysis program was used to fit binding isotherms for the crown:cation expected stoichiometry (N) of 1:1 for Na^+ binding. The binding constant obtained (log $K_S = 2.50$) is in the expected range. The data for K^+ complexation of **1** are shown in Figure 4. The instrument's internal program calculated binding constants for both $N = 1{:}1$ and 1:2 stoichiometries in the K^+ case. Although the latter is less intuitively appealing, the data fit is better (black line in Figure 4). To our knowledge, no explanation has been advanced to account for the calculated formation of 2:1 complexes between K^+ and an 18-membered crown, for which no 2:1 solid-state structures have been reported. The gray dashed line shows the less satisfactory fit calculated for a 1:1 stoichiometry, but the deviation is limited to the low concentration regime. Generally, the binding constants obtained by us using the ITC technique agreed with literature values where data are known. The method was then used to determine K_S for the naphthylmethyl-sidearmed compounds **4**·Na^+, **5**·Na^+, and **5**·K^+.

Several trends are apparent from the data in Table 1. First, the Na^+ and K^+ association constants for **1** (benzyl) and **5** (2-naphthylmethyl) are identical within experimental error. This is also true for the cation transport rates by these compounds as noted above. Second, the Na^+ association constants for **4** (1-naphthylmethyl) are lower than those for **1** or **5** by approximately 4-fold. Even though this moderate difference in equilibrium constants translates to only 0.8 kcal/mol relative energy difference, the effect is reproducible and is observed in both cation binding strengths and transport rates. This small energy difference is noteworthy because of the extremely subtle change in structure between **4** and **5**. The position of crown−sidearm attachment was not predicted to be important prior to the results reported here. The binding constants reported by Kubo for **6** (1-anthrylmethyl) are even lower than those for **4** in the one case where a direct comparison can be made (bottom row). Unfortunately, the nonstandard conditions (9:1 $CH_3OH/CHCl_3$)-

(32) Arnold, K. A.; Gokel, G. W. *J. Org. Chem.* **1986**, *51*, 5015−16.

required by solubility for determining the binding constant for **6** hamper our ability to draw a more meaningful conclusion.

The third set of observations concerns the magnitudes of the Na^+ and K^+ binding constants for **1**, **4**, and **5**. Compounds **4** and **5** are 1- and 2-naphthylmethyl isomers and the sterics of sidearm attachment are similar in **1** and **5** but not in **4**. The Na^+ binding and transport data for **1** and **5** are similar and higher than those for **4**. Specifically, binding constants (log K_S) for **1** and **5** are 2.50 and 2.37, respectively, and for **4**, the value is 1.87. The K^+ binding constants for **1**, **4**, and **5** are all in the range 3.27−3.55 although the anions are not identical (see Table 1). The most apparent difference is that although the binding of K^+ by **4** is poorer than that by **1** or **5**, the magnitude of the difference does not seem to be as large as observed for Na^+. To investigate further the K^+ binding properties, bulk membrane transport of K^+ was assessed for the isomeric 1- and 2-naphthyl crowns **4** and **5**. The experimental setup used was as described above except that potassium, rather than sodium, picrate was added to the source aqueous phase. Potassium transport was measured for **4** and **5** ($k = 1.2 \times 10^{-5}$ M/h, $\sim 7 \times 10^{-8}$ mol/h) and was found to be identical within experimental error. The fastest sodium transport rate, 5×10^{-6} M/h ($\sim 3 \times 10^{-8}$ mol/h), was observed for **1** (and **5**). Thus, the K^+ transport rate is significantly higher than that observed for Na^+ under otherwise identical conditions. The higher K^+ transport rates correlate to the higher K^+ binding constants as observed in previous studies.[31] As discussed below, the differences or similarities in binding affinity can be understood in terms of the solid-state structures of these compounds.

Solid-State Structures. The crystal structures of compounds **1**, **4**, **5**, and **6** are shown in Figure 5. The sidearms of these diaza-18-crown-6 compounds are benzyl (**1**), 1-naphthylmethyl (**4**), 2-naphthylmethyl (**5**), and 1-anthrylmethyl (**6**). Crystals of the uncomplexed crowns suitable for X-ray analysis were obtained from EtOH (**1**), acetone (**5**), and $CHCl_3$ (**6**). The structure of noncomplexed **4** is taken from a published report by Kubo and co-workers.[10] We have previously reported the structures of uncomplexed **1**,[33] **1**·NaI,[25] **4**·NaI,[25] **5**·NaI,[25] **6**·NaI_3,[26] and **6**·KSCN.[26] In Figure 5, the unbound compound is shown in the left column, and the Na^+ and K^+ complexes are shown in the center and right columns, respectively. The rows are organized according to the properties revealed in the present study. Compounds **1** and **5** (rows 1 and 2) show no unusual binding or transport properties and the solid-state conformations are as expected for these sidearms. Compounds **4** and **6** (rows 3 and 4) show reduced Na^+ binding and transport properties. The solid-state conformations of several of the Na^+ or K^+ complexes of these compounds are unusual and are described below.

Solid-State Conformations of Noncomplexed Macrocycles 1, 4, 5, and 6. The poor binding and transport properties exhibited by **4** and **6** suggested that the noncomplexed macrocycles might exhibit conformations dramatically different from those observed for good binders. This proved not to be the case. Instead, the structures of **1**, **4**, **5**, and **6** all show the macroring to be in the expected "parallelogram" conformation with the sidearms extended from the macroring nitrogen atoms to which they are attached. In benzyl-sidearmed **1**, 2-naphthylmethyl-sidearmed **5**, and anthrylmethyl-sidearmed **6**, macroring methylene groups adjacent to each ring nitrogen are rotated inward to occupy the molecular void inside the macrocycle. A minor variation is seen in the structure of **4** in which methylenes adjacent to oxygen (rather than nitrogen) atoms are rotated inward. In addition, the "parallelogram" of **4** is nearly square. As noted above, the sidearms in all four uncomplexed structures are extended away from the crown. No intramolecular interactions are observed between the macrocycle and any sidearm aromatic group.

Sodium and Potassium Complexed Macrocycles 1, 4, 5, and 6. Complexes of **1**, **4**, and **5** were obtained by dissolving equimolar amounts of the macrocycle and either NaI or KI in acetone and then allowing the crystals to grow by vapor diffusion with diethyl ether. Because of its low solubility, crystals of anthrylmethyl-sidearmed **6** were obtained from $CHCl_3$ (free **6**), THF (**6**·NaI_3 complex), and EtOH/$CHCl_3$ (1:1 v/v, **6**·KSCN complex).

Sodium Iodide Complexes of 1 and 5. The Na^+ complexes of **1** (R═CH_2Ph) and **5** (R═CH_2-2-Np) are identical in their essential features. In each case, the macroring is bowed upward with the nitrogen atoms located at the peaks. This invaginated conformation reduces the N↔N separation from ∼7.5 Å in the unbound macrocycle to ∼4.5 Å when Na^+ is complexed. Rather than being fully extended, the sidearms are also closer together: opposite methylenes are separated by 4.02 Å. The transannular sidearm methylene hydrogen atoms are separated by only 2.76 and 3.14 Å. The average Na^+-to-heteroatom distances are as expected. For **1** they are N−Na^+ = 2.64 ± 0.02 Å and O−Na^+ = 2.56 ± 0.2 Å, respectively. The corresponding values for **5** are N−Na^+ = 2.61 Å and O−Na^+ = 2.42 ± 0.01 Å. In the 2-naphthyl sidearm case (**5**), the aromatic residues reflect each other through a symmetry plane that intersects Na^+ and I^-. A similar structural situation is apparent for benzyl-sidearmed **1**, but the "mirror" is not a true symmetry plane.

In both cases, the iodide counterion is cradled between the arenes. One methylene hydrogen atom on each side is about 3.2 Å from iodide and in both cases the C−H−I angle is ∼165°. In neither case, however, is the iodide ion within the cation's solvation sphere.

Sodium Iodide Complex of 4. The structure observed for **4**·NaI is remarkably different from the isomeric complex **5**·NaI. First, the 1-naphthylmethyl sidearms of **4** are in an anti, rather than syn, arrangement with respect to the macrocycle, which is more nearly planar than in either **1**·NaI or **5**·NaI. Unlike the saddle-shaped macroring of **1**·NaI and **5**·NaI, the N↔N separation is significantly greater (5.9 Å). The average Na^+-to-heteroatom distances for **4** are typical: N−Na^+ = 2.76 ± 0.02 Å and O−Na^+ = 2.48 ± 0.06 Å.

The most noteworthy difference between the structures of isomeric naphthylmethyl-sidearmed **4** and **5** complexing NaI is that C−H···O interactions are apparent in the former. In both sidearms of **4**, a naphthalene α-hydrogen is separated from the nearest macroring oxygen atom by only (*d*) 2.67 Å (*D* = 3.56 Å) although their bond angles differ slightly. The two contacts are shown in Figure 6 in ORTEP representation superimposed on a tube structure. Note that the cation has been omitted to enhance clarity. The adjacent *β*-hydrogen (not shown in Figure 6) is 2.99 Å from the adjacent macroring nitrogen atom. This hydrogen also is only 3.31 Å from the iodide counterion but the angle of ∼149° leaves the significance of this interaction in doubt. The close contacts noted above, however, suggest significant C−H···O hydrogen bonding interactions.[21]

Sodium Iodide Complex of 6. The NaI_3 complex of **6** (R = CH_2An) is similar in general aspects to that of **4** (R = CH_2-1-Np) and quite different from the NaI complexes of **1** and **5**. As

(33) Arnold, K. A.; Viscariello, A. M.; Kim, M.; Gandour, R. D.; Fronczek, F. R.; Gokel, G. W. *Tetrahedron Lett.* **1988**, *29*, 3025−8.

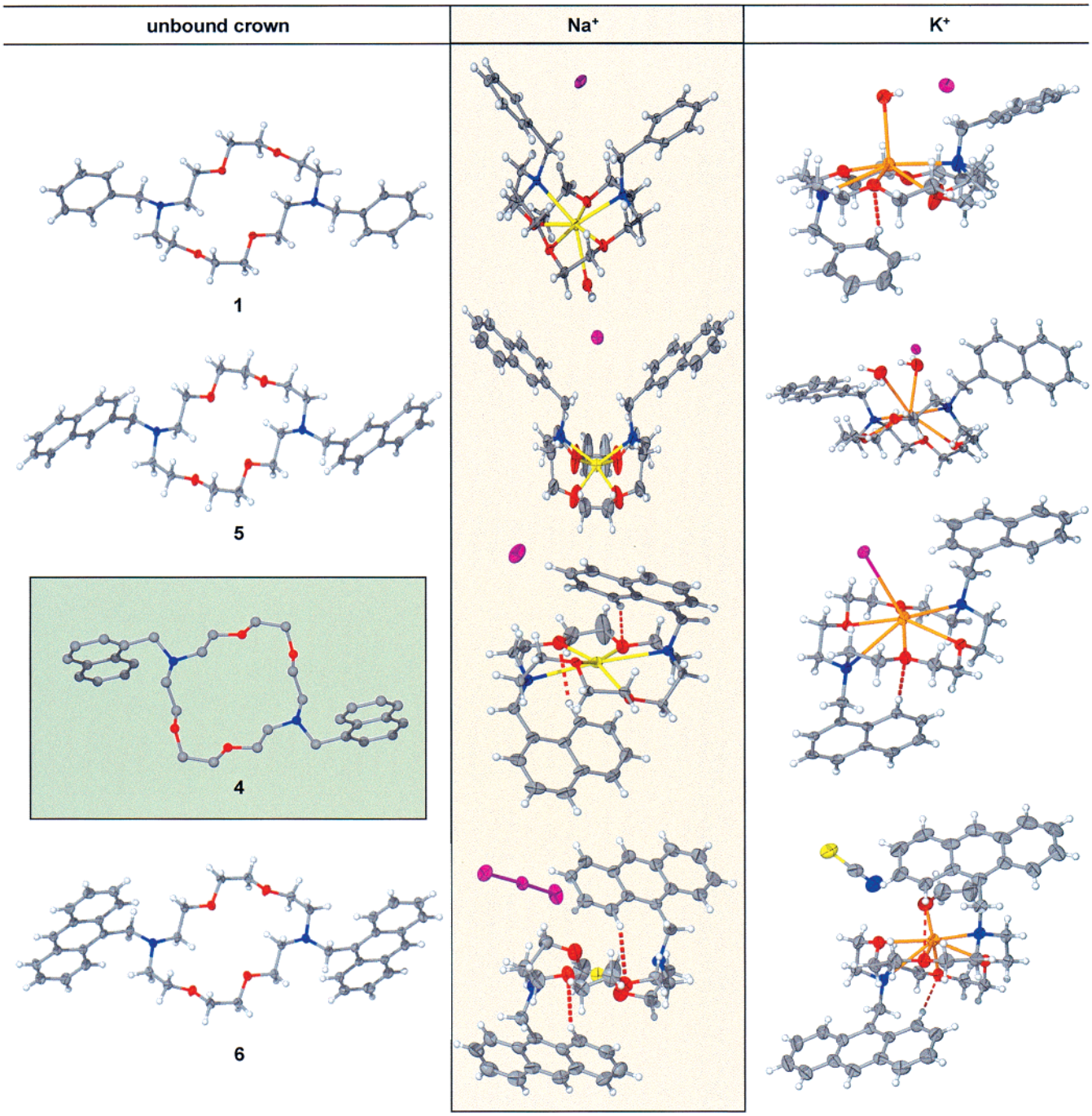

Figure 5. Solid-state structures of **1**, **4**, **5**, and **6** and their complexes with Na^+ and K^+. Column 1 (top to bottom): **1**, **5**, **4** (from ref 30), and **6**. Column 2: **1**·NaI·H_2O, **5**·NaI, **4**·NaI, and **6**·NaI_3. Column 3: **1**·KI·H_2O, **5**·KI·$2H_2O$, **4**·KI and **6**·KSCN.

in the case of **4**·NaI, the macroring is in an approximately D_{3d} conformation. The average Na^+−O distance is 2.46 ± 0.05 Å and the Na^+−N distances are 2.92 and 3.03 Å. These values are longer than those observed in the **4**·NaI case but not unusual for diaza-18-crown-6·Na^+ complexes. The sidearms are in the anti, rather than the syn, conformation. This sidearm orientation effectively screens the anion from the cation's solvation sphere. Essentially the same situation was observed for **4**·NaI but the larger size of the anthryl residues screens the macroring more completely.

The anthryl rings are involved in intramolecular C−H···O contacts. Two of the peri hydrogens in **6**·NaI_3 are within van der Waals contact distance of crown oxygens. The C−H···O contacts observed in **6**·NaI_3 are illustrated in Figure 7. The arrangement of the interacting atoms is nearly identical with those in **4**·NaI: $D = 3.55 \pm 0.02$ Å and $\theta = 155 \pm 2°$.

Two THF molecules were also present in the crystal lattice of **6**·NaI_3. Remarkably, these normally strong donor oxygens of THF do not coordinate the ring-bound cation. Indeed, the THF molecules are disordered in the lattice and their dipoles do not obviously point to any cation. Triiodide counterion likewise does not coordinate the ring-bound Na^+ cation. The apical coordination sites of Na^+ are apparently rendered inaccessible to THF or the counterion by the proximity of the anthrylmethyl sidearms.

Potassium Iodide Complex of 1. A previous structure for a KSCN complex of **1** (R = CH_2Ph) showed a typical crown conformation with the macroring in a D_{3d} conformation and

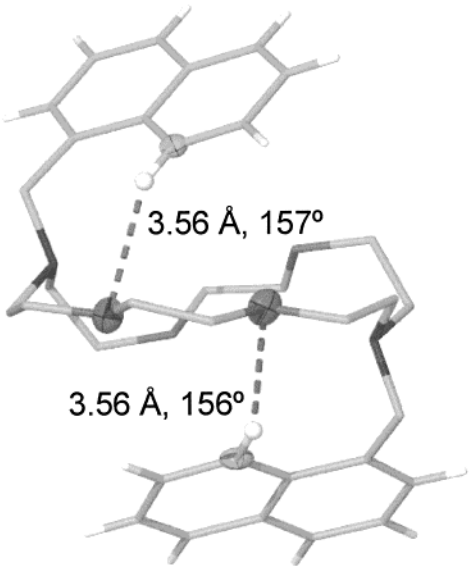

Figure 6. C−H···O interactions in the crystal structure of **4**·NaI. Note that some atoms are not shown for clarity.

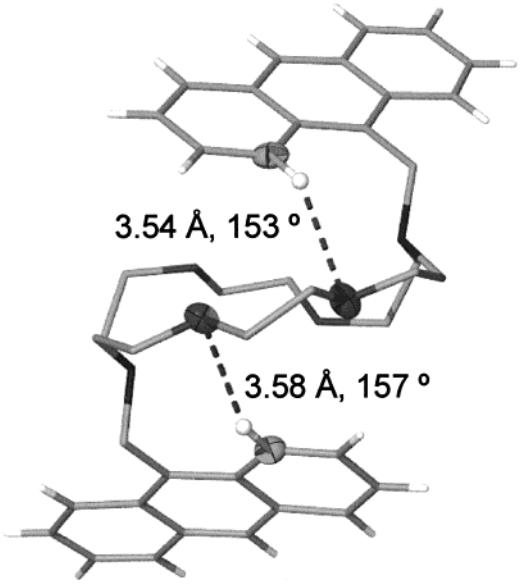

Figure 7. C−H···O interactions in the crystal structure of **6**·NaI_3. Note that some atoms are not shown for clarity.

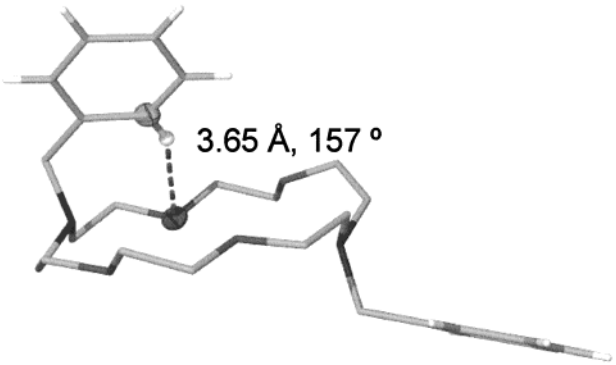

Figure 8. C−H···O interaction in the crystal structure of **1**·KI·H_2O. Note that some atoms are not shown for clarity.

the sidearms extended to either side of the ring.[33] We report here a new K^+ complex structure for the compound having the stoichiometry **1**·KI·H_2O (see Figure 8). This new complex differs primarily in sidearm orientation; the macroring has an approximate D_{3d} conformation. The average K^+−O distance is 2.84 ± 0.1 Å while the average K^+−N distance is 3.0 ± 0.1 Å.

The benzyl sidearms are oriented very differently in **1**·KI·H_2O than they are in **1**·KSCN. Figure 8 illustrates the arrangement of the relevant atoms for the former (K^+ is again omitted for clarity). One of the sidearms in **1**·KI·H_2O is positioned such that the benzyl methylene is turned toward the macroring and the phenyl group is turned away from it. The planes of the arene and macroring are approximately parallel, intersecting at an angle of ∼25°. The other benzyl sidearm is folded over the crown and the *o*-hydrogen is involved in a close C−H···O contact. The C···O distance (D = 3.65 Å) and angle (θ = 157°) are clearly in accord with a CH···O hydrogen bond.

The unusual sidearm conformation can be accounted for by the C−H···O interaction between sidearm and macroring. This interaction does not, however, prevent solvent (H_2O) from coordinating the ring-bound cation. A single molecule of water was clearly located at the superior apical position of the potassium ion. The K^+−O (water) distance is 2.85 Å.

The structure of **1**·KI·H_2O clearly differs from that of **1**·KSCN although the basic crown macroring binding interactions are similar. In solution, of course, binding of solvated K^+ should be similar. A previous report suggested that anion dependent changes in cation transport and selectivity are due to differences in anion shape and thus the crown's ability to coordinate the cation.[34] An alternate hypothesis is suggested by the structures here. Differences in the anion may manifest themselves in conformational changes within the complexing agent. Of course, the host molecules presented here are more complicated than dicyclohexano-18-crown-6, the subject of the previous study.

Potassium Iodide Complex of 5. The KI complex of **5** (R = CH_2-2-Np) was found to have the stoichiometry **5**·KI·$2H_2O$. The macrocycle adopts a saddle-shaped conformation which is similar to that found in **5**·NaI and **1**·NaI although it is less bowed (see Figure 5). The bowed conformation contracts the ring so that the average K^+−N distance is 2.91 ± 0.01 Å. The average K^+−O (crown) distance of 2.82 ± 0.08 Å is typical of 18-membered-ring potassium complexes and similar to those reported here. In addition to the macroring donors, two water molecules coordinate potassium cation in a syn arrangement (K^+−O distance = 2.86 ± 0.12 Å). Potassium is thus 8-coordinate in this structure. No intramolecular C−H···O interactions could be identified in this structure.

Potassium Iodide Complex of 4. The complex of **4** (R = CH_2-1-Np) is unique among the structures reported here in that it contains an anion in the first coordination sphere of the alkali metal cation. The crown is in approximately the D_{3d} conformation and the average K^+−heteroatom distances are typical: K^+−O, 2.75 ± 0.11 Å and K^+−N, 3.2 ± 0.2 Å. The K^+−I distance is 3.62 Å. Potassium cation is 7-coordinate in this complex.

The orientation of the sidearms is similar in **1**·KI and **4**·KI. One of the α-naphthyl groups in **4**·KI is extended from the macroring while the other is folded back toward it. This is shown in Figure 9, which illustrates the C−H···O interaction involving the naphthalene sidearm. The naphthalene α-hydrogen of the folded sidearm is close (D = 3.66 Å) to a crown oxygen. In this case, the hydrogen bond is almost linear: θ = 179° suggesting a favorable and significant contact.

Potassium Thiocyanate Complex of 6. The macrocycle in **6**·KSCN is approximately in the D_{3d} conformation (as observed for **1**·KI·H_2O, **4**·NaI, and **6**·NaI_3). The average K^+-to-oxygen

(34) Olsher, U.; Hankins, M. G.; Kim, Y. D.; Bartsch, R. A. *J. Am. Chem. Soc.* **1993**, *115*, 3370−3371.

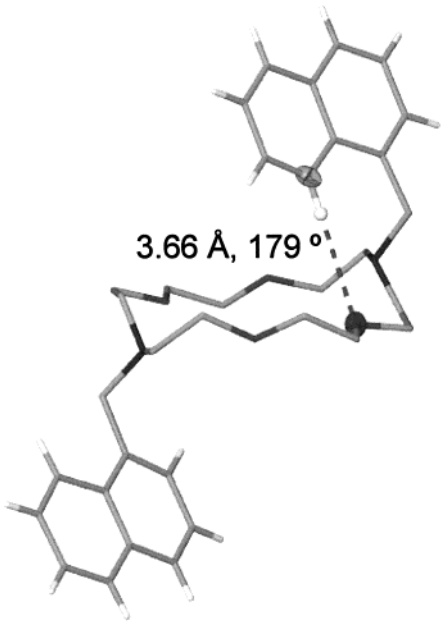

Figure 9. C−H···O interaction in the crystal structure of **4**·KI. Note that some atoms are not shown for clarity.

distance in the macrocycle is 2.73 ± 0.05 Å and the average K^+-to-macrocycle nitrogen distance is 3.2 ± 0.2 Å. Two molecules of ethanol are also present in the asymmetric unit cell. The hydroxyl oxygen of one of the alcohol molecules coordinates to the ring-bound K^+ ion. The K^+−O distance in this case is 2.71 Å, about the same as that for the macroring oxygen donors. The K^+ cation is thus 7-coordinate. The four ring oxygens, one molecule of ethanol, and one of the nitrogen atoms (K^+−N distance 2.96 Å) provide the major solvation. The second nitrogen atom appears to interact more weakly as judged by the greater K^+−N distance of 3.40 Å. The second molecule of ethanol and the SCN^- counterion do not interact at all with the K^+ cation.

The most interesting feature of the **6**·KSCN complex is the presence of close C−H···O contacts similar to those observed in the structures discussed above. The C···O distances (D) are 3.58 and 3.63 Å, and the angles (θ) are 177.5° and 155.5°, respectively. An additional close contact worth noting occurs between carbon-3 of one of the anthryl groups and the sulfur atom of the SCN^- anion, D = 4.12 Å and θ = 151.3°.

Summary of Functional and Structural Data. The aromatic-sidearmed lariat ethers have been characterized functionally by

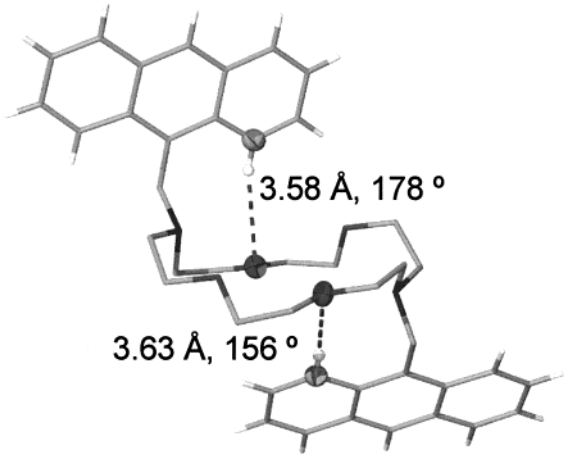

Figure 10. C−H···O interactions in the crystal structure of **6**·KSCN. Note that some atoms are not shown for clarity.

determining Na^+ and K^+ transport rates through a bulk organic liquid membrane and by measurement of homogeneous cation binding constants. The results obtained from the binding and transport studies correlate reasonably well, as we have observed for single-armed lariats.[31]

The binding and transport studies revealed quite surprising differences in the ability of certain of these aromatic crowns to transport Na^+. The most revealing case involves isomeric **4** and **5**. Their binding constants and transport rates differ significantly even though they are isomers. Such a difference is not observed, however, for the K^+ transport rates (essentially identical) and binding constants (similar, see Table 1) for these two isomeric crowns. Although solid-state data may not accurately reflect the situation in solution, they are often extremely informative. One interaction that is generally apparent in the solid-state structures is an intramolecular C−H···O hydrogen bond.

Clear evidence has been found and presented above for C−H···O interactions in unbound **3** and **7**. Aromatic C−H interactions with macroring oxygen atoms are observed in Na^+·**4** and Na^+·**6**. The K^+ complexes of **1**, **4**, and **6** all show significant C−H···O interactions as well. In cases where at least two C−H···O interactions are observed, the transport rate and binding constant for Na^+ are clearly affected. In contrast, when no or only one close C−H···O interaction is apparent, cation binding strengths and transport rates are about as expected. Isomeric crowns **4** and **5**, which exhibit similar K^+ transport rates and binding constants, lack "interference" or "competition" resulting from intramolecular C−H···O hydrogen bonding (there is only one C−H···O interaction present in K^+·**5** and none in K^+·**4**). In contrast, the more "encumbered" Na^+ complexes differ significantly from each other. Thus, normal binding is observed for **5** with Na^+ but very poor binding is observed in Na^+·**4** and Na^+·**6**, both of which exhibit strong C−H···O H-bond interactions.

We speculate that the H-bond induced organization of the sidearms hinders access of the cation to the macroring, poor cation access that is reflected in low cation binding constants and transport rates. The difference in macroring conformation required by K^+ compared to Na^+ subtly alters the sidearm orientation, the formation of H-bonds, and thus the efficacy of cation binding. The ability of C−H···O contacts to affect binding is apparent in the structure of the unbound crown **7** (as well as **3**, see Figure 2). The organization of an arene group over each face of the macrocycle makes the ring inaccessible to Na^+ or K^+. A C−H···O contact also renders two potential donor oxygens in the macrocycle inaccessible for binding. When the sidearms are H-bonded as described above, their lack of flexibility constitutes steric hindrance to entry and egress of the cation and/or solvent.

C−H···O Interactions in Proteins: Myoglobin. A fundamental goal in studies such as those presented here is to use bioorganic chemistry to probe individual interactions that may be difficult to observe or assess in the protein context. Clearly, proteins are rife with oxygen (backbone carbonyl, aspartic acid, asparagine, glutamic acid, glutamine, serine, threonine, and tyrosine). The abundance of the C−H···O contacts in the solid-state structures of these simple macrocycles suggested that such interactions are likely to be general and to extend to the biochemical context. Indeed, nearly 10% of all amino acids in proteins contain aromatic side chains. We were particularly interested in the aromatic rings of Phe, Tyr, and Trp. Histidine was not considered because the pK_A of imidazole is in the physiological range. If the aromatic hydrogens on Phe, Tyr, and Trp can favorably interact with crown ether oxygen atoms, then

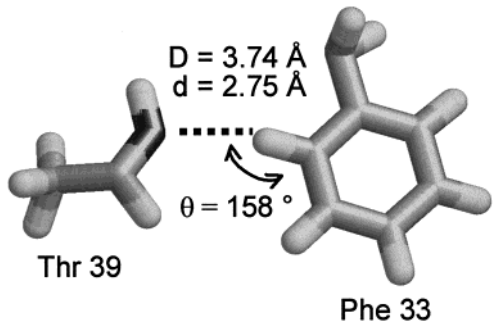

Figure 11. C−H···O interaction observed in the crystal structure of myoglobin from a neutron diffraction analysis study. Structure taken from PDB entry 2MB5.[36a]

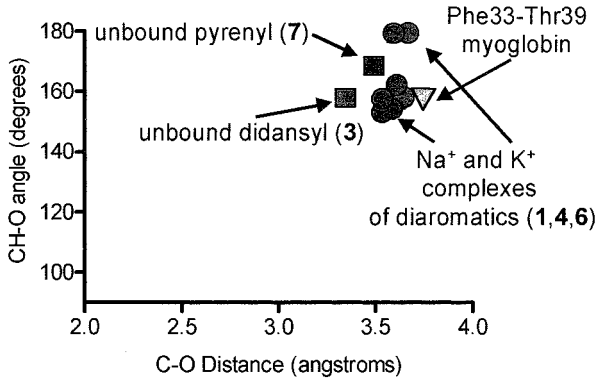

Figure 12. Geometry of the C−H···O interactions found in the crystal structures of diazacrown ethers having aromatic sidearms. The C−H···O interaction from myoglobin (shown in Figure 11) is also included for comparison.

it should also be possible to find related examples in the crystal structures of at least some proteins. To our knowledge the first work of this type was that of Thomas et al.,[20c] who reported a statistical preference for the edge, rather than the face, of phenylalanine side chains to pack near oxygen atoms in protein structures. Although this work was clearly important, specific examples of close aromatic-oxygen interactions in proteins were lacking in the paper.

We designated carbonyl oxygens or the side chain oxygen atoms of Ser, Thr, or Tyr as H-bond acceptors in our search. The ability to identify specific examples of C−H···O interactions in proteins presents a challenge because protein structures normally have resolutions >2.0 Å. At this level of resolution, hydrogen atoms cannot be precisely located. We therefore decided to limit our initial efforts to reports for which neutron diffraction data were available.

Myoglobin was the first protein to be solved by X-ray crystallography[35] and a structure has also been determined based on neutron diffraction data.[36] We surveyed the aromatic residues in the neutron diffraction structure of myoglobin (PDB code 2MB5) and discovered several close C−H···O contacts involving aromatic rings. Figure 11 illustrates one of the examples. A C−H···O contact is apparent between a phenylalanine (F33) C−H and the threonine hydroxyl (T39). The angle ($\theta = 158°$) and distances ($D = 3.74$ Å, $d = 2.76$ Å) are similar to the many C−H···O interactions described above.

The close C−H···O contact in myoglobin is reminiscent of the interactions observed in the small molecule receptors reported here. A scatter plot of the distances and angles for these complexes is shown in Figure 12. The myoglobin example has also been included for comparison. The distances are clustered between 3.3 and 3.7 Å and the angles between 155° and 180°. These values fall within the ranges designated by Desiraju.[21]

Conclusion

Two important findings have emerged from the present study. First, at the fundamental chemical level, considerable additional evidence has been found for C−H···O interactions. These interactions are significant by current criteria. Interesting as their existence may be, the correlation between structure, transport dynamics, and cation binding strengths within a closely related family of structures is of even greater import. Finding numerous clear interactions of this type in a well-characterized family of compounds suggests that other species may reveal similar contacts. The second point is that we have identified the analogous interaction in a published protein crystal structure. We feel confident that many more examples will emerge when sought and that higher resolution structures will show that, in aggregate, C−H···O hydrogen bonds are important interactions in peptides, proteins, and perhaps other highly organized biological systems.

Experimental Section

Infrared spectra were recorded on a Perkin-Elmer 1310 infrared spectrophotometer (KBr unless otherwise noted) and were calibrated against the 1601 cm^{-1} band of polystyrene. Melting points were determined on a Thomas-Hoover apparatus in open capillaries and are uncorrected. Thin layer chromatographic (TLC) analyses were performed on silica gel HLO F-254 (0.25 mm thickness), Scientific Adsorbents, Inc. Commercial starting materials and solvents were purified, as appropriate, by using standard techniques prior to use. For the crystallizations, commercially available solvents and salts were used without further purification.

***N,N′*-Bis(benzyl)-4,13-diaza-18-crown-6 (1)** was prepared as previously described.[27] The compound used in these studies had a melting point and physical properties identical with those previously described.

***N,N′*-Bis(2-hydroxybenzyl)-4,13-diaza-18-crown-6 (2)** was prepared as previously described.[28] The compound used in these studies had a melting point and physical properties identical with those previously described.

***N,N′*-Bis(dansyl)diaza-18-crown-6 (3)** was prepared as previously described.[12] The compound used in these studies had a melting point and physical properties identical with those previously described.

***N,N′*-Bis(1-naphthylmethyl)-4,13-diaza-18-crown-6 (4)** was prepared as previously described.[25] The compound used in these studies had a melting point and physical properties identical with those reported by Kubo.[9]

***N,N′*-Bis(2-naphthylmethyl)-4,13-diaza-18-crown-6 (5)** was prepared as previously described.[25]

***N,N′*-Bis(1-anthrylmethyl)-4,13-diaza-18-crown-6 (6)** was prepared as previously described.[26] The compound used in these studies had a melting point and physical properties identical with those reported by Kubo.[10]

Bulk Membrane Transport. The concentric tube method was as previously described.[31,37] In brief, a chloroform layer separated two aqueous phases. The source phase consisted of a 1 mM solution of sodium picrate or potassium picrate which was prepared by dissolving picric acid in 0.100 M NaOH or KOH. The receiving phase was initially

(35) (a) Kendrew, J. C.; Bodo, G.; Dintzis, H. M.; Parrish, H.; Wyckoff, H.; Phillips, D. C. *Nature* **1958**, *181*, 662−666. (b) Kendrew, J. C.; Dickerson, R. E.; Strandberg, B. E.; Hart, R. J.; Phillips, D. C.; Shore, V. C. *Nature* **1960**, *185*, 422−427.

(36) (a) Cheng, X.; Schoenborn, B. P. *J. Mol. Biol.* **1991**, *220*, 381−99. (b) Cheng, X.; Schoenborn, B. P. *Acta Crystallogr.* **1990**, *B46*, 195−199. (c) Schoenborn, B. P. *Nature* **1969**, *224*, 143−6.

(37) Murillo, O.; Suzuki, I.; Abel, E.; Murray, C. L.; Meadows, E. S.; Jin, T.; Gokel, G. W. *J. Am. Chem. Soc.* **1997**, *119*, 5540−5549.

distilled, deionized water. A layer of 6.0 mL of $CHCl_3$ (1.0 mM in ionophore) was stirred (Magne-4 synchronous stirrer, 100 rpm) using a 7 mm stir bar. The 10 mm glass tube separated the source (1 mL) and receiving (6 mL) phases in a 20 mL beaker. The internal diameter of the tube was 10 mm. The transport rate of sodium or potassium picrate was calculated from the picrate concentration in the receiving phase. The picrate concentration was determined by measuring the absorbance ($\lambda = 354$ nm) of a diluted 250 μL aliquot from the aqueous receiving phase. UV−visible spectra were recorded on a Beckman DU-8 spectrophotometer.

Binding Constant Determination. The method used was identical with that reported previously,[32] except as noted. The sodium electrode was a Ross Model 8411. The reference was a Model 476370 Corning double junction electrode. The electrodes were checked for Nerstian response prior to use and the method was verified by determining the binding constant of dibenzyldiaza-18-crown-6 (**1**) which was within experimental error to the value determined previously.

Isothermal Titration Calorimetry. The OMEGA calorimeter from MicroCal[38] was used. The sample cell (1.7 mL) was filled with the crown solution at a concentration of 2−10 mM in methanol. The temperature was maintained at 25 ± 0.1 °C. The injection syringe, equipped with a stirring paddle, had a volume of 250 μL and was rotated at 400 rpm. The injections were normally 5 μL and were completed every 5 min. The titrant was a methanolic salt solution, typically 100 mM NaI or KI. The methanol was anhydrous from Aldrich. The NaI or KI was dried in a vacuum oven at 100 °C for a minimum of 1 week prior to preparing the titration solution.

X-ray Crystallography. Intensity data for **6** were collected at 298 K on a Siemens P4 diffractometer (2θ scan mode, Cu Kα radiation, $\lambda = 1.5418$ Å). Data for all other crystals reported here were collected at 173(1) K on a Bruker SMART CCD diffractometer (**a** scan mode Mo Kα radiation, $\lambda = 0.7107$ Å). Data were corrected for absorption using the program SADABS.[39] Structure solution and refinement proceeded similarly for all structures (SHELX-97 software[40] using the X-Seed[41] interface). Direct methods yielded all non-hydrogen atoms of the asymmetric unit. These atoms were refined anisotropically (full-matrix least-squares method on F^2). Hydrogen atoms were placed in calculated positions with their isotropic thermal parameters riding on those of their parent atoms. When structures required modeling of disorder, the disordered hydrogen atoms were not placed. All X-ray structure figures were prepared with X-Seed and POV-Ray.[42]

Crystal Data. The structures of **1**,[33] **3**,[12] **4**,[9] and **7**[11] were taken from published reports.

Crystal data for **1**·NaI·H_2O: $M = 610.49$; colorless rhombohedroids, 0.30 × 0.25 × 0.25 mm^3; tetragonal, $P\bar{4}21c$; $a = 21.2891(8)$ Å, $b = 21.2891(8)$ Å, $c = 12.1557(6)$ Å; $Z = 8$; $V = 5509.3(4)$ Å^3; $D_c = 1.472$ g/mm^3; $2\theta_{max} = 54.4°$, 31676 reflections collected, 6072 unique ([R(int) = 0.0608]); final GoF = 0.902, $R1 = 0.0305$, $wR2 = 0.0589$, R indices based on 5238 reflections with $I > 2\sigma(I)$, Lp and absorption corrections applied, $\mu = 1.216$ mm^{-1}, minimum transmission factor = 0.7118.

Crystal data for **1**·KI·H_2O: $M = 617.59$; colorless rhombohedroids, 0.35 × 0.35 × 0.10 mm^3; monoclinic, $C2/c$; $a = 25.9720(18)$ Å, $b = 9.4521(7)$ Å, $c = 23.8259(17)$ Å, $\beta = 100.4530(10)°$; $Z = 8$; $V = 5751.9(7)$ Å^3; $D_c = 1.426$ g/mm^3; $2\theta_{max} = 54.22°$, 17359 reflections collected, 6346 unique [R(int) = 0.0441]; final GoF = 0.903, $R1 = 0.0323$, $wR2 = 0.0625$, R indices based on 4151 reflections with $I > 2\sigma(I)$, $\mu = 1.292$ mm^{-1}, minimum transmission factor = 0.6606.

Crystal data for **2**: $M = 542.70$; colorless rhombohedroids, 0.35 × 0.30 × 0.15 mm^3; triclinic, $P\bar{1}$; $a = 7.1374(16)$ Å, $b = 9.307(2)$ Å, $c = 10.839(3)$ Å, $\alpha = 90.845(4)°$, $\beta = 105.008(4)°$, $\gamma = 112.040(4)°$; $Z = 1$; $V = 639.6(3)$ Å^3; $D_c = 1.232$ g/mm^3; $2\theta_{max} = 54.26°$, 3962 reflections collected, 2728 unique [R(int) = 0.0211]; final GoF = 1.063, $R1 = 0.0425$, $wR2 = 0.1129$, R indices based on 1977 reflections with $I > 2\sigma(I)$, $\mu = 0.087$ mm^{-1}, minimum transmission factor = 0.9702.

Crystal data for **4**·NaI: $M = 692.59$; colorless rhombohedroids, 0.30 × 0.25 × 0.20 mm^3; triclinic, $P\bar{1}$; $a = 10.3046(6)$ Å, $b = 12.3433(7)$ Å, $c = 12.8362(7)$ Å; $\alpha = 93.3770(10)°$, $\beta = 98.3800(10)°$, $\gamma = 97.0350(10)°$. $Z = 2$; $V = 1598.17(16)$ Å^3; $D_c = 1.439$ g/Mm^3; $2\theta_{max} = 54.26°$, 9539 reflections collected, 6592 unique [R(int) = 0.0151]; final GoF = 1.023, $R1 = 0.0464$, $wR2 = 0.1258$, R indices based on 5431 reflections with $I > 4\sigma(I)$, $\mu = 1.055$ mm^{-1}, minimum transmission factor = 0.7129.

Crystal data for **4**·KI; $M = 708.70$; colorless rhombohedroids, 0.35 × 0.30 × 0.15 mm^3; orthorhombic, P 21 21 21; $a = 7.4024(4)$ Å, $b = 10.5893(6)$ Å, $c = 41.829(3)$ Å; $Z = 4$; $V = 3278.8(3)$ Å^3; $D_c = 1.436$ g/mm^3; $2\theta_{max} = 54.36°$, 20626 reflections collected, 7268 unique [R(int) = 0.0450]; final GoF = 0.963, $R1 = 0.0367$, $wR2 = 0.0603$, R indices based on 5622 reflections with $I > 2\sigma(I)$, $\mu = 1.143$ mm^{-1}, minimum transmission factor = 0.6905.

Crystal data for **5**: $M = 542.70$; colorless rhombohedroids, 0.45 × 0.30 × 0.25 mm^3; triclinic, $P\bar{1}$; $a = 7.3907(8)$ Å, $b = 10.2449(11)$ Å, $c = 11.1461(13)$ Å, $\alpha = 62.749(2)°$, $\beta = 80.022(2)°$, $\gamma = 87.014(2)°$; $Z = 1$; $V = 738.57(14)$ Å^3; $D_c = 1.220$ g/mm^3; $2\theta_{max} = 54.26°$, 4664 reflections collected, 3189 unique [R(int) = 0.0163]; final GoF = 1.046, $R1 = 0.0448$, $wR2 = 0.1195$, R indices based on 2402 reflections with $I > 2\sigma(I)$, $\mu = 0.079$ mm^{-1}, minimum transmission factor = 0.7118.

Crystal data for **5**·NaI: $M = 692.59$; colorless rhombohedroids, 0.30 × 0.25 × 0.25 mm^3; orthorhombic, $Pnma$; $a = 12.7957(9)$ Å, $b = 21.1947(15)$ Å, $c = 11.9900(8)$ Å; $Z = 8$; $V = 3251.7(4)$ Å^3; $D_c = 1.415$ g/mm^3; $2\theta_{max} = 54.4°$, 19444 reflections collected, 3697 unique [R(int) = 0.0487]; final GoF = 1.056, $R1 = 0.0590$, $wR2 = 0.1535$, R indices based on 1873 reflections with $I > 2\sigma(I)$, Lp and absorption corrections applied, $\mu = 1.037$ mm^{-1}, minimum transmission factor = 0.7129.

Crystal data for **5**·KI·$2H_2O$: $M = 744.73$; colorless rhombohedroids, 0.35 × 0.25 × 0.20 mm^3; monoclinic, $P21/c$; $a = 12.1173(6)$ Å, $b = 11.5332(6)$ Å, $c = 24.9629(13)$ Å, $\beta = 93.5970(10)°$; $Z = 4$; $V = 3481.7(3)$ Å^3; $D_c = 1.421$ g/mm^3; $2\theta_{max} = 54.26°$, 21161 reflections collected, 7695 unique [R(int) = 0.0227]; final GoF = 1.040, $R1 = 0.0374$, $wR2 = 0.0839$, R indices based on 2402 reflections with $I > 2\sigma(I)$, $\mu = 1.084$ mm^{-1}, minimum transmission factor = 0.7029.

Crystal data for **6**: $M = 642.81$; yellow plates, 0.50 × 0.40 × 0.10 mm^3; triclinic, $P\bar{1}$; $a = 7.7128(6)$ Å, $b = 9.6455(9)$ Å, $c = 11.7605(7)$ Å, $\alpha = 91.322(7)$, $\beta = 93.916(6)$, $\gamma = 102.368(8)°$; $Z = 1$; $V = 851.97(12)$ Å^3; $D_c = 1.253$ g/mm^3; $2\theta_{max} = 133.94°$, 6772 reflections collected, 2923 unique [R(int) = 0.0563]; final GoF = 1.056, $R1 = 0.0644$, $wR2 = 0.1551$, R indices based on 1854 reflections with $I > 4\sigma(I)$, $\mu = 0.63$ mm^{-1}.

Crystal data for **6**·NaI_3·2THF: $M = 1190.71$; yellow-brown rhombohedroids, 0.45 × 0.30 × 0.20 mm^3; triclinic, $P\bar{1}$; $a = 10.4883(5)$, $b = 14.9523(8)$, $c = 15.9911(8)$ Å, $\alpha = 89.275(1)°$, $\beta = 86.012(1)°$, $\gamma = 79.708(1)°$; $Z = 2$; $V = 2461.5(2)$ Å^3; $D_c = 1.607$ g/cm^3; $2\theta_{max} = 54.5°$, 14255 reflections collected, 9894 unique ($R_{int} = 0.0402$); final GoF = 0.976, $R1 = 0.0736$, $wR2 = 0.1876$, R indices based on 6222 reflections with $I > 2\sigma(I)$, Lp and absorption corrections applied, $\mu = 1.963$ mm^{-1}, minimum transmission factor = 0.530.

Crystal data for **6**·KSCN·2EtOH: $M = 832.12$; colorless rhombohedroids, 0.40 × 0.25 × 0.25 mm^3; monoclinic, $P2_1/n$; $a = 13.5604(7)$ Å, $b = 19.6871(10)$ Å, $c = 16.4820(8)$ Å, $\beta = 105.098(1)°$; $Z = 4$; $V = 4248.2(4)$ Å^3; $D_c = 1.301$ g/cm^3; $2\theta_{max} = 54.4°$, 24296 reflections collected, 9212 unique ($R_{int} = 0.0277$); final GoF = 1.061, $R1 = 0.0606$, $wR2 = 0.1476$, R indices based on 6625 reflections with $I > 2\sigma(I)$, Lp and absorption corrections applied, $\mu = 0.227$ mm^{-1}, minimum transmission factor = 0.808.

Acknowledgment. We thank the NIH (GM-36262) and the NSF (CHE-9805840) for grants that supported this work. We are also grateful for an ACS Division of Organic Chemistry fellowship, funded by Procter and Gamble, to E.S.M. We appreciate helpful discussions with Prof. Normand Voyer and thank Prof. Jeffrey Gordon and Dr. J. Michael Bradshaw for use of the titration calorimeter.

JA9940672

(38) Wiseman, T.; Williston, S.; Brandts, J. F.; Lin, L.-N. *Anal. Biochem.* **1989**, *179*, 131−137.

(39) Blessing, R. H. *Acta Crystallogr.* **1995**, *A51*, 33−8.

(40) Sheldrick, G. M., 1997, University of Göttingen.

(41) Barbour, L. J., 1999, University of Missouri-Columbia. (http://www.lbarbour.com/xseed/).

(42) http://www.povray.org.